Organic Geochemistry 178 (2023) 104582

Contents lists available at ScienceDirect

Organic Geochemistry

journal homepage: www.elsevier.com/locate/orggeochem

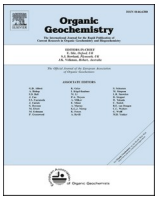

# Isoprenoidal GDGTs and GDDs associated with anoxic lacustrine environments

Danica Mitrović [a,*], Ellen C. Hopmans [a], Nicole J. Bale [a], Nora Richter [a,b], Linda A. Amaral-Zettler [a,b,c], Allix J. Baxter [d], Francien Peterse [d], Pedro Miguel Raposeiro [e,f], Vítor Gonçalves [e,f], Ana Cristina Costa [e,f], Stefan Schouten [a,d]

[a] NIOZ Royal Netherlands Institute for Sea Research, Department of Marine Microbiology and Biogeochemistry, P.O. Box 59, 1790 AB Den Burg, the Netherlands
[b] Department of Earth, Environmental and Planetary Sciences, Brown University, 324 Brook Street, Providence, Rhode Island 02912, USA
[c] Department of Freshwater and Marine Ecology, Institute for Biodiversity and Ecosystem Dynamics, University of Amsterdam, the Netherlands
[d] Utrecht University, Department of Earth Sciences, Faculty of Geosciences, Princetonlaan 8a, 3584 CD Utrecht, the Netherlands
[e] CIBIO Centro de Investigação em Biodiversidade e Recursos Genéticos, InBIO Laboratório Associado, Pólo dos Açores, Rua da Mãe de Deus, 9500-321 Ponta Delgada, Portugal
[f] Faculdade de Ciências e Tecnologia, Universidade dos Açores, Rua da Mãe de Deus, 9500 321 Ponta Delgada, Portugal

ARTICLE INFO

Associate Editor: Prof Isla Castaneda

*Keywords:*
S-GDGTs
S-GDDs
Lacustrine anoxia
Sediments
UHPLC-HRMS
Messel oil shale
Azorean lakes
Lake Chala

ABSTRACT

We examined membrane-spanning archaeal lipids using ultra high pressure liquid chromatography-high resolution mass spectrometry (UHPLC-HRMS) in a suite of sediment samples from both cored sequences (Messel oil shale and Lake Chala) and surface sediments (Azorean lakes) encompassing ancient and modern (Eocene to Present) lacustrine environments. Additionally we compared the lacustrine data to those of marine (Mediterranean cored sequences, Arabian Sea surface sediments and Monterey outcrop sediments) and hypersaline sediments (Vena del Gesso marls) as well as marine suspended particulate matter (SPM) from the Black Sea. Regular isoprenoidal glycerol dialkyl glycerol tetraethers (GDGTs) and glycerol dialkyl diethers (GDDs) were the most abundant membrane-spanning lipids in all investigated settings (>90 % and 84 % respectively). Interestingly, GDGTs with a cyclohexyl ring (S-GDGTs) were also present in almost all investigated lake sediments, in relative abundances of ca. 2–7 % and, for the first time, also their S-GDD counterparts were detected (2–10 %). The producers of S-GDGTs are still unknown, however our results show that it is likely that bottom water anoxia (both seasonally induced or permanent) is the driving factor for the production of these lipids, whereas previous studies suggested euxinia was required for production. Unsaturated GDGTs (*uns*-GDGTs, ca. 2 %) were only detected in Lake Chala sediments and surface sediments from Azorean lakes, but without accompanying *uns*-GDDs. GMGTs, glycerol monoalkyl glycerol tetraethers, were present in Messel oil shale and marine samples, while GMDs were only found in Messel oil shale.

## 1. Introduction

Archaea are widespread in both the marine water column and in underlying sediments (Brocks and Pearson, 2005; Lipp and Hinrichs, 2009; Spang et al., 2017; Summons et al., 2021) where they play important roles in global biogeochemical cycles such as the methane and nitrogen cycles (Boetius et al., 2000; Pancost et al., 2001; Könneke et al., 2005; Francis et al., 2007; Jarrell et al., 2011). They are also widespread in lacustrine environments, where they perform a similar function (Glissman et al., 2004; Bomberg et al., 2008; Auguet et al., 2010; Vuillemin et al., 2018). Archaeal membranes are characterized by isoprenoidal glycerol ether lipids, mainly *sn*-2,3-diphytanyl glycerol diethers with two $C_{20}$ phytanyl chains (archaeol) or *sn*-2,3-dialkyl diglycerol tetraethers with two glycerol moieties connected by two $C_{40}$ isoprenoid chains (glycerol dialkyl glycerol tetraethers [GDGTs], which can contain 0 to 8 cyclopentane moieties [i.e., GDGT-n, where n is the number of cyclopentane moieties]; cf. Fig. 1) (e.g., De Rosa and Gambacorta, 1988; Koga et al., 1993; Gambacorta et al., 1995; Sinninghe Damsté et al., 2002). Soon after their discovery, it was suggested that isoprenoidal ether lipids could provide an advantage in extreme

* Corresponding author.
*E-mail address:* danica.mitrovic@nioz.nl (D. Mitrović).

https://doi.org/10.1016/j.orggeochem.2023.104582
Received 12 November 2022; Received in revised form 14 February 2023; Accepted 27 February 2023
Available online 2 March 2023

environments (high temperature, high salinity, or extreme pH), on the basis that they are more chemically stable than the ester-linked membrane lipids present in Bacteria and Eukarya (Langworthy, 1977; Thompson et al., 1992; Kates, 1993). However, the discovery of widespread occurrence of GDGTs in non-extreme environments (Schouten et al., 2000a), in concert with the cosmopolitan detection of archaeal DNA (e.g., Fuhrman et al., 1992; De Long 1992), threw doubt on this hypothesis. Schouten et al. (2002) first suggested that the number of cyclopentane moieties in isoprenoidal GDGTs within marine sediments was related to sea surface temperature (SST), and developed the $TEX_{86}$ index (TetraEther indeX of 86 carbons) as a paleothermometer applicable to marine sediment sequences. Since then the $TEX_{86}$ index has been used to reconstruct SST over the past 190 million years of Earth history (Inglis et al., 2015; O'Brien et al., 2017).

Developments in liquid chromatography-mass spectrometry (LC-MS) methodology (e.g., Hopmans et al., 2000; Wörmer et al., 2013, 2015) have facilitated the subsequent discovery and tentative identification of a wide range of GDGTs other than the 'regular' GDGTs (i.e., GDGT 0–8). For example, Liu et al. (2012c) described a range of novel hydroxy isoprenoidal ether lipids in marine sediments, the OH-GDGTs, which were thought to mainly originate from planktonic archaea (Huguet et al., 2013; Elling et al., 2014). OH-GDGT based indices show potential as a tool to reconstruct past surface water temperature in polar regions (e.g., Yermak Plateau close to the Arctic Ocean: Kremer et al., 2018; Prydz Bay in Antarctica: Liu et al., 2020). Glycerol monoalkyl glycerol tetraethers (GMGTs; also referred to as H-shaped GDGTs) were first reported in the hyperthermophilic methanogen *Methanothermus fervidus* (Morii et al., 1998; Koga and Morii, 2005) and the thermophilic euryarchaeote *Aciduliprofundum boonei* (Schouten et al., 2008a). Naafs et al. (2018) showed that GMGTs may be used as paleotemperature indicators in tropical peats and immature coals (lignite) from mid-latitude regions. Unsaturated GDGTs (*uns*-GDGTs) have been reported in a suite of marine environments by Zhu et al. (2014) and, based on their abundances and distributions, the authors suggested that they constitute an important archaeal lipid group in euxinic basins (the Black Sea Basin) and an investigated cold seep site (site off the coast of Pakistan, in which focused upward migration of methane stimulates high rates of anaerobic oxidation of methane). Uns-GDGTs were also reported in the lacustrine surface sediment of a meromictic marl lake (Fayetteville Green Lake, near Syracuse in New York: Liu et al. 2016a). Unsaturations have been frequently reported in diphytanyl glycerol diethers (DGDs, e.g., archaeol), where the proportion of *uns*-DGDs in cultured halophilic archaea increases with increasing ambient NaCl concentration (Maestrojuan et al., 1992; Hafenbradl et al., 1993; Dawson et al., 2012). However, reports of *uns*-GDGTs in marine and lacustrine sediments are relatively sparse. Biphytanes which contain a cyclohexane ring, instead of ones with the more commonly reported cyclopentane ring, were first described by Chappe et al. (1980) and Chappe (1982) after HI-degradation (refluxing with hydroiodic acid in order to release and analyse the ether-bound hydrocarbon skeletons of GDGTs) of Messel oil shale lacustrine sediments. The GDGTs containing these biphytane moieties were first reported by Liu et al. (2016a) in surface sediment from Fayetteville Green Lake (FGL), the Messel pit (horizon between 2.5 and 3.5 m), sediments from Salt Pond, Woods Hole salt marshes at Trunk River (41°32′4.8″N, 70°38′30.4″W) and Little Sippewissett marsh (41°34′33.5″N, 70°38′14.9″W). These were named S-GDGTs (where 'S' stands for both 'sulfidic' and 'six-membered ring') as they were hypothesized to be produced by chemoautotrophic archaea that live in euxinic conditions.

In the past decade, glycerol dialkyl diether (GDD; cf. Fig. 1), analogues to several GDGT classes have also been tentatively identified. Regular GDDs have been observed in marine subsurface sediments from various geological settings (e.g., the Mediterranean Sea, margins of Peru, Namibia, Cascadia etc. by Liu et al., 2012a) and Mediterranean sediments from the Messinian period (Knappy and Keely, 2012), OH-GDDs in marine (Liu et al., 2012b) and coastal wetlands (Lü et al., 2019), and GMDs, the diether analogues of GMGTs, in sediments deposited under hydrothermal conditions (surface sediments from the Red Sea; Bauersachs and Schwark, 2016). It has been postulated that GDDs are either degradation products of GDGTs or biosynthesized by

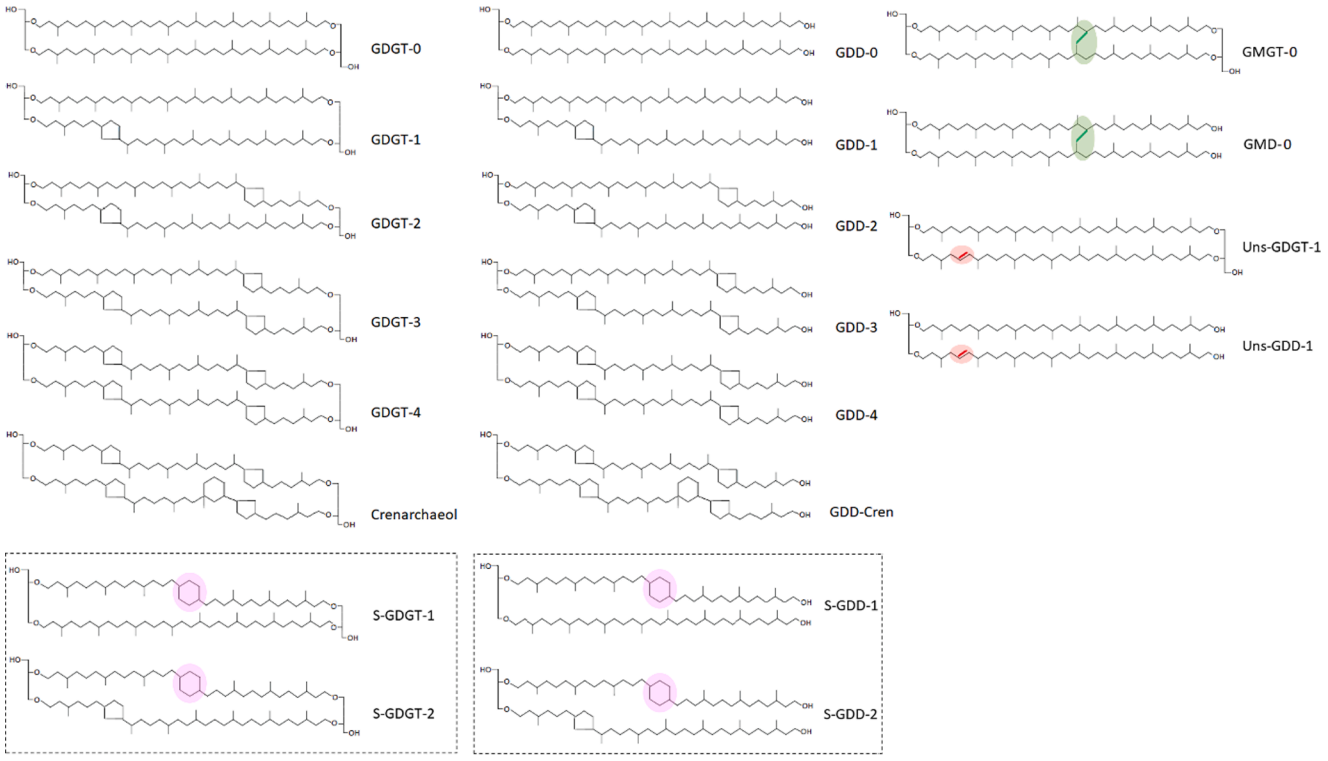


**Fig. 1.** Structures of membrane-spanning archaeal lipids: regular isoprenoid GDGTs (-0 to Cren); S-GDGTs; H-shaped (GMGTs & GMDs) and unsaturated (uns-GDGT-1 & uns-GDD-1) GDGTs and GDDs. Note: the position of bridge in H-shaped and double bond in unsaturated GDGTs/GDDs is speculative.

archaea, either as membrane components or as GDGT intermediates (Liu et al., 2012a; Yang et al., 2014; Meador et al., 2014; Coffinet et al., 2015; de Bar et al., 2019).

In this study we examined GDGT and GDD diversity in a range of recent and ancient lacustrine settings that are either seasonally or permanently anoxic as well as in various anoxic marine settings using ultra high pressure liquid chromatography-high resolution mass spectrometry (UHPLC-HRMS). We specifically focused our study on those GDGTs and GDDs whose occurrence has been linked to anoxia, to further constrain their use as potential proxies for anoxic environmental conditions.

## 2. Materials and methods

### 2.1. Samples and study sites

We analysed sediment cores from two geographically distinct crater lakes characterized by permanent anoxia (Messel paleolake in Germany and Lake Chala in Kenya) as well as modern surface sediments from a variety of lakes (of volcanic origin and other natural depressions) from the Azores Archipelago. For comparison, sediments (both core and surface) and suspended particulate matter (SPM) from several marine environments characterized by anoxia or anoxic events were also studied (cf. Table S1 for the full list of samples).

#### 2.1.1. Lakes

***Messel oil shale.*** Messel paleolake is an ancient maar crater lake that was formed by a phreatomagmatic eruption (Felder and Harms, 2004). The samples for this study (n = 18) were obtained from a core drilled in the Messel oil shale sequence (borehole number 5 – Darmstadt, Germany; Matthess, 1966; Rullkötter et al., 1988; Franzen and Schaal, 2000) that is Middle Eocene in age (47.8 Ma; Mertz and Renne, 2005; Lenz et al., 2011). It is noteworthy that Messel paleolake in the Middle Eocene was ~ 46° – 47°N, therefore experiencing a tropical climate (Grein et al., 2011). The total organic carbon content (TOC) of Messel oil shale is 27 % on average (Bauersachs et al., 2014).

***Azorean lakes.*** Surface sediment samples (n = 18) from seven Azorean lakes and one coastal lagoon in the mid-Atlantic Azores Archipelago (Portugal) were analyzed. The Azores are particularly rich in lentic habitats, with 88 lakes (Porteiro, 2000), ranging between 0.4 m (Lagoa do Caldeirão Norte on São Miguel Island) and 115 m depth (Lagoa Negra on Flores Island), respectively. The lower water column of the deeper lakes is known to experience seasonal anoxia (i.e., depletion of oxygen in the bottom waters due to temperature gradient that stratifies the water column during summer months) (Gonçalves, 2008; Ribeiro et al., 2014; Raposeiro et al., 2018; Ritter et al., 2022). Surface sediments were collected during a sampling campaign in 2018 and stored at -40 °C at the NIOZ. TOC, as determined in this study, varied between 4 % (Lake Azul on São Miguel Island) and 21 % (Lake Lomba on Flores Island).

***Lake Chala.*** Lake Chala (Kenya/Tanzania) is a permanently-stratified (meromictic) tropical crater lake (Verschuren et al., 2009; Buckles et al., 2014, 2016). In September 2016 the International Continental Scientific Drilling Program (ICDP) project DeepCHALLA (Verschuren et al., 2013) recovered a continuous sediment sequence spanning the last ca. 250 kyr (Martin-Jones et al., 2020; Maitituerdi et al., 2022) from below its profundal zone. For this study, 168 samples from the core were examined (~20 – 63 m and 119 – 190 m) of which 14 % contain turbidites (sediments originating from a more peripheral location that end up at the drill site after bottom-slope failure; cf. Table S1 for full list of samples).

#### 2.1.2. Marine and hyper saline sediment and suspended particular matter

***Monterey Formation.*** Marine sediments from the Miocene Monterey Formation (n = 10; 5.9 – 18.4 Ma, Schouten et al., 2000b, c; Isaacs et al., 2001; Isaacs and Rullkötter, 2001) were investigated. These sediments are outcrop samples from the Naples Beach section, California (USA) obtained in 1989 and 1990 in the framework of the Cooperative Monterey Organic Geochemistry Study (CMOGS) (Isaacs, 1992). Based on the integrative CMOGS geological and palaeontological analysis, sediments from Naples Beach represent a unique occurrence (Isaacs and Rullkötter, 2001 and references therein). TOC varied between 1 and 17 % (Isaacs and Rullkötter, 2001).

***Sapropels.*** Eastern Mediterranean sapropel sediments from the Pleistocene, ranging in age from 121.5 to 128 kyr BP were analysed (n = 12; S5; Rush et al., 2019; Bale et al., 2019a). These sediments were sampled from a piston core taken at a water depth of 1760 m in the eastern part of the basin (Levantine Basin) (core 64PE406-E1) on R/V *Pelagia* in 2016. TOC content is up to 12 %.

***Western Mediterranean.*** Western Mediterranean sediment core sampled at Station 8 (core 64PE407-W8) (n = 3; Weiss et al., 2019) at 1963 m water depth. The core was retrieved during a cruise 64PE407 on R/V *Pelagia* in 2016.

***Arabian Sea.*** Arabian Sea surface sediments from various water depths (900 – 3000 m) collected from the Murray Ridge in the Arabian Sea in January 2009 (n = 3; Lengger et al., 2012).

***Vena del Gesso.*** Marls were analysed from the Vena del Gesso outcrop (Gessoso-solfifera formation) deposited during the Mediterranean Miocene salinity crisis (n = 12; Messinian – 7.2 Ma, Vai and Ricci Lucchi, 1977; Sinninghe Damsté et al., 1995). Vai and Ricci Lucchi (1977) identified 14 distinguishable evaporitic cycles (i.e., beds) that formed in the Vena del Gesso Basin; the samples investigated in this study belong to four different cycles, namely the most developed bed IV, beds V, VII and XI. The TOC ranges from 1.2 to 2.5 %.

***Black Sea water column.*** SPM (n = 15) was analysed from the suboxic and euxinic redox zones of the Black Sea obtained during two cruises in 2013 (PHOXY cruise; 100 to 2000 m water depth) and 2017 (64PE418 cruise; 90 to 2000 m water depth) on board of R/V *Pelagia* (Bale et al., 2021; Ding et al., 2021).

### 2.2. Sample extraction

The majority of the samples were extracted using a modified Bligh-Dyer (BD) method (Sturt et al., 2004; with additional modifications described in Bale et al., 2021). Samples extracted for this study include Messel oil shales, the Azorean lake surface sediments, Vena del Gesso marls, Monterey sediments, Western Mediterranean sediment core and Arabian Sea surface sediments. The Mediterranean sapropels and Black Sea SPM were extracted as described in previous studies (Rush et al., 2019; Bale et al., 2019a; Bale et al., 2021). A mixture of methanol: dichloromethane:phosphate buffer (MeOH:DCM:PB 2:1:0.8, v:v) was used for ultrasonic extraction (2 × 10 min) and combined supernatants were phase-separated by adding DCM and PB to obtain a final solvent ratio of 1:1:0.9 (v:v). The organic phase containing the intact polar lipids (IPLs) was collected and the aqueous phase re-extracted three times with DCM. The whole extraction process was then repeated on the residue but with a mixture of MeOH:DCM:TCA (aqueous trichloroacetic acid solution; pH 3; 2:1:0.8, v:v). The organic extracts were combined and dried under a stream of $N_2$ gas. Before analysis the extracts were redissolved in a mixture of MeOH:DCM (9:1, v:v) and filtered through 0.45 μm regenerated cellulose syringe filters (4 mm diameter; Grace Alltech).

The Lake Chala sediments have been extracted previously in the same manner as described for the Lake Chala sediments (core depths between 60 and 65 m) in Baxter et al. (2019). Briefly, extraction was done using ASE Dionex$^{TM}$ apparatus with a DCM:MeOH mixture 9:1 (v:v) at high temperature (100 °C) and pressure (7.6 × $10^6$ Pa). The total lipid extracts (TLEs) were first dissolved in a small amount of DCM/methanol (v:v 1:1) and run on a $Na_2SO_4$ column to remove the excess water and dried under $N_2$ gas. TLEs were than separated into apolar, ketone and polar fractions using $Al_2O_3$ column chromatography with eluents *n*-hexane:DCM (9:1, v:v), *n*-hexane:DCM (1:1, v:v) and DCM:MeOH (1:1, v:v), respectively. All Chala polar fractions were dried under

$N_2$ gas and filtered using a PTFE 0.45 μm filter. The polar fractions were analysed for the purpose of this study.

### 2.3. Hydrogenation

Selected acid-hydrolysed Bligh Dyer (BD) extracts of Messel oil shale sediments (from 72 and 76 m core depth; Table S1), as well as a polar fraction of one surface sediment from Lake Azul (SS4; Table S1) were hydrogenated to aid in the identification of unsaturated GDGTs. Hydrogenation was done in ethyl acetate (EtOAc) with 1 drop of concentrated acetic acid by bubbling $H_2$ over $PtO_2$ as catalyst (Aldrich) for 1 h at room temperature, followed by overnight stirring (Schouten et al., 2008a).

### 2.4. Elemental analyses

TOC, total nitrogen ($N_{tot}$) and total sulfur ($S_{tot}$) contents were measured for the Azorean lake surface sediments (n = 18). The analysis was done on decalcified, powdered and freeze-dried samples (ca. 30 mg for lakes Azul and Verde, ~10 mg all others) using an Elementar Vario Isotope Cube directly linked to an Isotope Ratio Mass Spectrometer (IRMS) Elementar Isoprime vision. Samples for TOC analysis were pretreated with excess 2 M hydrochloric acid (HCl) to remove carbonates and were put on a shaker overnight. They were then neutralized with bidistilled water and freeze-dried. TOC was measured in duplicate with a sample reproducibility of < 0.5 %.

### 2.5. Ether lipid analysis

Analysis of both the BD extracts and polar fractions was carried out using UHPLC-HRMS according to Wörmer et al. (2013), with modifications described in Bale et al. (2021). Briefly, analysis was carried out on an Agilent 1290 Infinity I UHPLC, equipped with thermostatted autoinjector and column oven, coupled to a Q Exactive Orbitrap MS with a Ion Max source and heated electrospray ionization (HESI) probe (Thermo Fisher Scientific). Separation was achieved on an Acquity BEH C18 column (Waters, 2.1 × 150 mm, 1.7 mm) maintained at 30 °C. The eluent composition was (A) methanol/water/formic acid/14.8 M $NH_3$aq [85:15:0.12:0.04 (v:v)] and (B) isopropyl alcohol/methanol/formic acid/14.8 M $NH_3$aq [50:50:0.12:0.04 (v:v)]. The elution program was: 95 % A for 3 min, followed by a linear gradient to 40 % A at 12 min and then to 0 % A at 50 min, this was maintained until 80 min. The flow rate was 0.2 mL $min^{-1}$. Positive ion HESI settings were: capillary temperature, 300 °C; sheath gas ($N_2$) pressure, 40 arbitrary units (AU); auxiliary gas ($N_2$) pressure, 10 AU; spray voltage, 4.5 kV; probe heater temperature, 50 °C; S-lens 70 V. Lipids were detected using a mass range of *m/z* 350 – 2000 and $MS^2$ spectra were obtained via data-dependent acquisition, where the top ten abundant ions per $MS^1$ scan were selected for fragmentation. Additionally, dynamic exclusion (6.0 s) was used as well as an inclusion list containing calculated *m/z* values for all known GDGTs and GDDs. Stepped normalized collision energy (NCE) of 15, 22.5 and 30 was used for fragmentation. Distributions of GDGTs and GDDs were determined by integration of peak area of the summed mass chromatograms of the protonated, ammoniated and sodiated molecules ($[M + H]^+$, $[M + NH_4]^+$, $[M + Na]^+$) and their first isotopologue within 3 ppm relative mass tolerance.

### 2.6. Indices and Statistics

The ring indices of GDGTs, GDDs, S-GDGTs and S-GDDs were calculated using a modified equation of He et al. (2012). The ratios and calculations that were carried out on the core lipid data are as follows:

Ring index GDGTs =

$$\frac{(\%\text{GDGT-1}) + (\%\ \text{S-GDGT-1}) + 2*(\%\text{GDGT-2}) + 2*(\%\text{S-GDGT-2}) + 3*(\%GDGT-3) + 4*(\%GDGT-4) + 5*(\%Crenarchaeol)}{100}$$

and Ring index GDDs =

$$\frac{(\%GDD-1) + (\%S-GDD-1) + 2*(\%GDD-2) + 2*(\%S-GDD-2) + 3*(\%GDD-3) + 4*(\%GDD-4) + 5*(\%Cren-GDD)}{100}$$

Principal component analysis was performed using R (version R-4.0.4; R Core Team, 2021) using factoextra (version 1.0.7; Kassambara and Mundt, 2020) on calculated relative abundances of regular, H-shaped, *uns*- and S-GDGTs and GDDs.

## 3. Results & discussion

### 3.1. Identification of GDGTs and GDDs

A broad range of regular isoprenoidal GDGTs and GDDs were detected in all settings (cf. Fig. 1 for structures and nomenclature). GDGTs and GDDs were tentatively identified based on their elution patterns under reversed phase chromatography (Liu et al., 2016a) and by comparison with published fragmentation spectra (Knappy et al. 2009, 2011; Knappy and Keely 2012; Liu et al., 2012b, c; Zhu et al., 2014; Bauersachs and Schwark, 2016). Fig. 2 shows the distribution of GDGTs and GDDs in a Lake Messel oil shale (79 m; Fig. 2a) and in Lake Azul surface sediment (SS4; Fig. 2b). In addition to the regular GDGTs 1–4 and crenarchaeol, several early and late eluting isomers of various GDGTs were observed (Fig. 2a, b). S-GDGT-1 (with one cyclohexyl moiety; $MS^2$ in Fig. S1b) and S-GDGT-2 (with one cyclopentyl and one cyclohexyl moiety) elute after GDGT-1 and −2 respectively (Fig. 2), as described by Liu et al. (2016a). The extracted ion chromatograms of *m/z* 1300.307 and 1298.291 also contained a series of peaks eluting before GDGT-1 and GDGT-2. GMGT-0, −1 and −2 (Fig. 2a) were identified based on comparison of their fragmentation spectrum to published spectra (Schouten et al., 2008a; Knappy et al., 2009; Bauersachs and Schwark, 2016). Spectra of GMGTs are characterized by a series of losses of $H_2O$ (−18) from their protonated molecule and a lack of fragments relating to the loss of one of the isoprenoid chains. Liu et al. (2016a) identified early eluting peaks as unsaturated GDGTs (*uns*-GDGTs), with a reversed elution order compared to the regular GDGTs. As *uns*-GDGTs cannot be distinguished from GDGTs with ring structures in the isoprenoid chains based on mass spectrometry, selected samples were hydrogenated to confirm their identification (Fig. S2). Peaks that were no

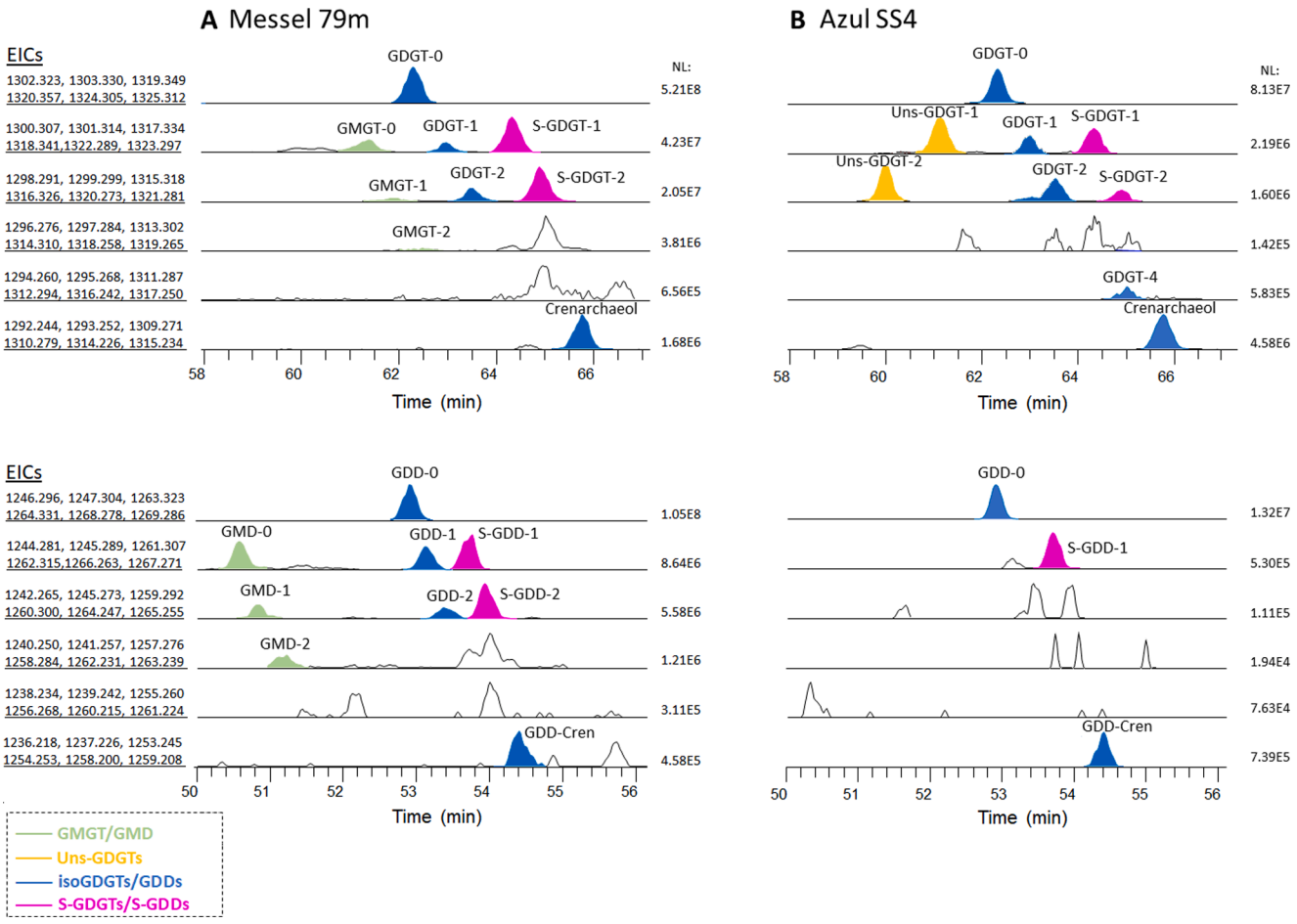


**Fig. 2.** Partial summed Extracted Ion Chromatograms (EIC), showing elution patterns of GDDs and GDGTs under reverse phase (RP) conditions with accurate masses of protonated, ammoniated and sodiated adducts (and their first isotopologue) indicated, of Messel oil shale sediment (79 m) (A) and Lake Azul surface sediment (SS4) (B). Structures of detected ether lipids are shown in Fig. 1. All chromatograms were smoothed with a factor Gaussian 7. NL: corresponds to Normalization Level of peak intensity.

longer detected after hydrogenation were thus identified as *uns*-GDGTs (Fig. S2b). The early eluting isomers in Messel were identified as GMGTs, while in Azul they were identified as *uns*-GDGTs. The *uns*-GDGTs observed in Azul conform to the elution pattern designated as 0:1:0 and 0:2:0 by Liu et al. (2016a) (*uns*-GDGT-1 and *uns*-GDGT-2, respectively; Fig. 1 for structures and nomenclature). This assignment complies with x:y:z naming system where x represents the number of cyclopentyl rings, y the number of double bonds and z the number of cyclohexyl rings in GDGT structure, as described in Liu et al. (2016a).

In addition to the GDGTs described above, various GDDs were detected in all investigated sediments. The distribution of GDDs in a Messel oil shale and Azul sediments largely followed the distribution of GDGTs (cf. example in Fig. 2). In addition to the regular GDDs (labelled GDD-0 to GDD-Cren; Fig. 2a, b), both a series of late and early eluting peaks were observed. The distribution of the late eluting peaks mirrored that of the S-GDGTs and they were identified as S-GDDs based on their later retention time compared to the regular GDDs, as well as their $MS^2$ spectra. The $MS^2$ spectrum of S-GDD-1 (0:0:1; Fig. S1a) exhibited an [M

**Table 1**
Relative abundances (%) and standard deviations of GDGTs (GDDs), GMGTs (GMDs), S-GDGTs (S-GDDs) and *uns*-GDGTs in examined samples.

| Samples | | Type | GDGTs | GMGTs | S-GDGTs | Uns-GDGTs | GDDs | GMDs | S-GDDs |
|---|---|---|---|---|---|---|---|---|---|
| **Lakes** | | | | | | | | | |
| Messel (n = 18) | | Lacustrine oil shale | 90.2 ± 5.9 | 2.7 ± 1.8 | 7.2 ± 4.3 | – | 84.1 ± 8.9 | 5.5 ± 3.6 | 10.4 ± 5.8 |
| Lake Chala (n = 168) | | Sediment core | 95.0 ± 2.5 | – | 2.8 ± 1.6 | 2.1 ± 1.2 | 97.9 ± 2.1 | – | 2.1 ± 2.1 |
| Azorean lakes (n = 18) | | Surface sediment | 95.9 ± 3.5 | – | 1.8 ± 1.3 | 2.3 ± 2.3 | 94.1 ± 4.0 | – | 5.9 ± 4.0 |
| **Marine/hypersaline** | | | | | | | | | |
| Monterey(Naples Beach) (n = 10) | | Miocene marine sediments | 99.8 ± 0.2 | 0.2 ± 0.2 | – | – | 100 | – | – |
| E. Mediterranean (n = 12) | | Pleistocene sapropel | 100 | – | – | – | 100 | – | – |
| W. Mediterranean (n = 3) | | Sediment core | 100 | – | – | – | 100 | – | – |
| Arabian Sea (n = 3) | | Surface sediment | 100 | – | – | – | 100 | – | – |
| Vena del Gesso (n = 12) | bed IV, V, VII & XI | Hypersaline marls | 97.1 ± 1.9 | 2.5 ± 1.5 | 0.4 ± 0.6 | – | 100 | – | – |
| **Suboxic/euxinic marine** | | | | | | | | | |
| Black Sea (n = 15) | | SPM[a] | 100 | – | – | – | 100 | – | – |

[a] SPM – Suspended Particulate Matter.

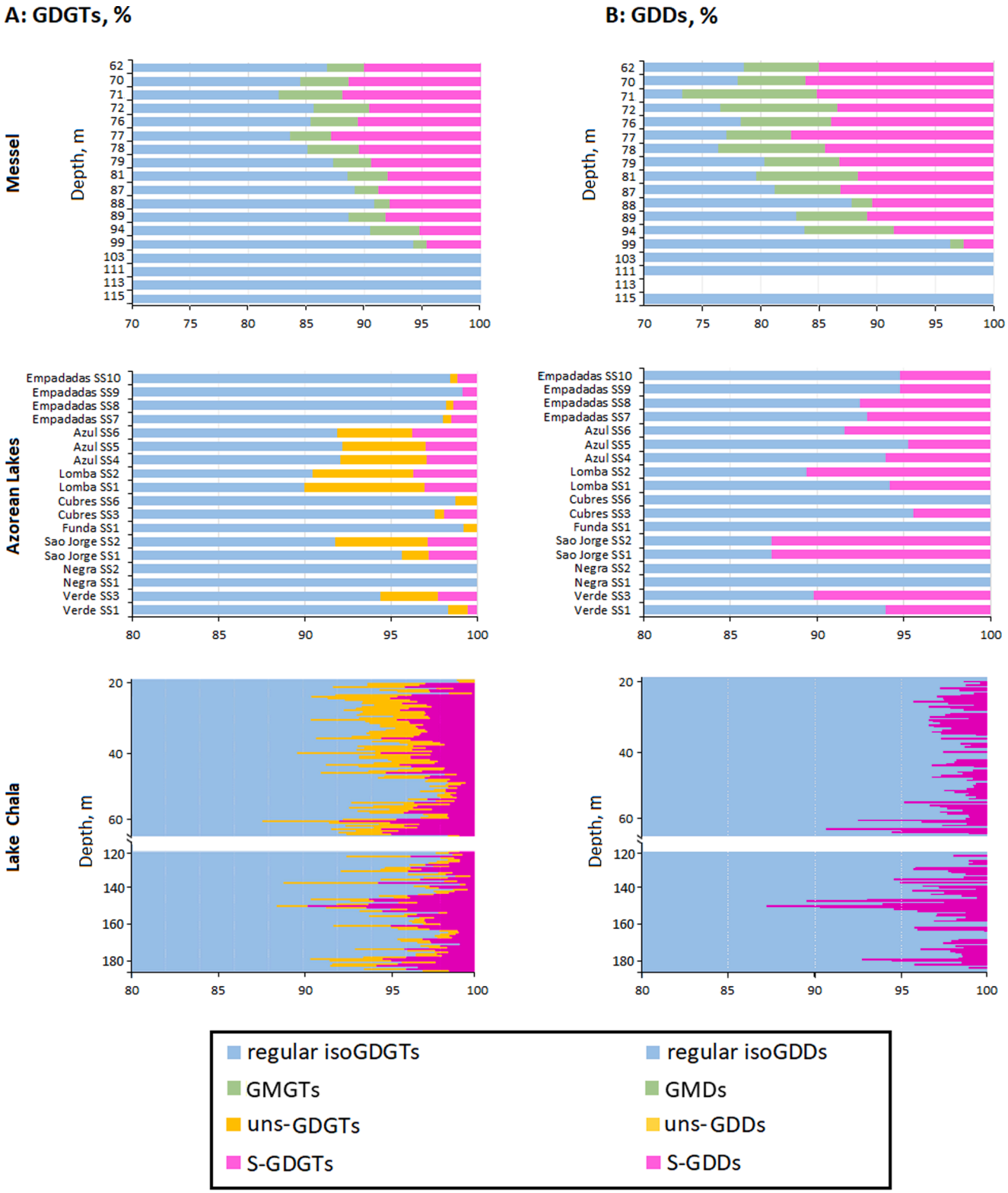


**Fig 3.** Relative distributions (%) of all GDGTs (A) and GDDs (B) identified in Messel oil shale sediments, Azorean lakes surface sediments and investigated Lake Chala core sediments.

+ H]$^+$ ion at *m/z* 1244.281 and [M + H-$H_2O$]$^+$ at *m/z* 1226.270. Additional diagnostic fragments included a fragment ion at *m/z* 667.660 which represents the loss of 576.620 ($C_{40}H_{80}O$; an alkyl chain with ring, presumably the cyclohexane ring). To the best of our knowledge this represents the first report of S-GDDs.

GMDs, diether analogues of GMGTs, were identified based on their retention time and comparison with published spectra (Bauersachs and Schwark, 2016). The $MS^2$ spectrum of GMD-0 contained a [M + H]$^+$ ion at *m/z* 1244.281, with the only significant fragment ions at *m/z* 1226.270 and 1208.259 representing sequential losses of water. The presence of *uns*-GDDs could not be unambiguously confirmed.

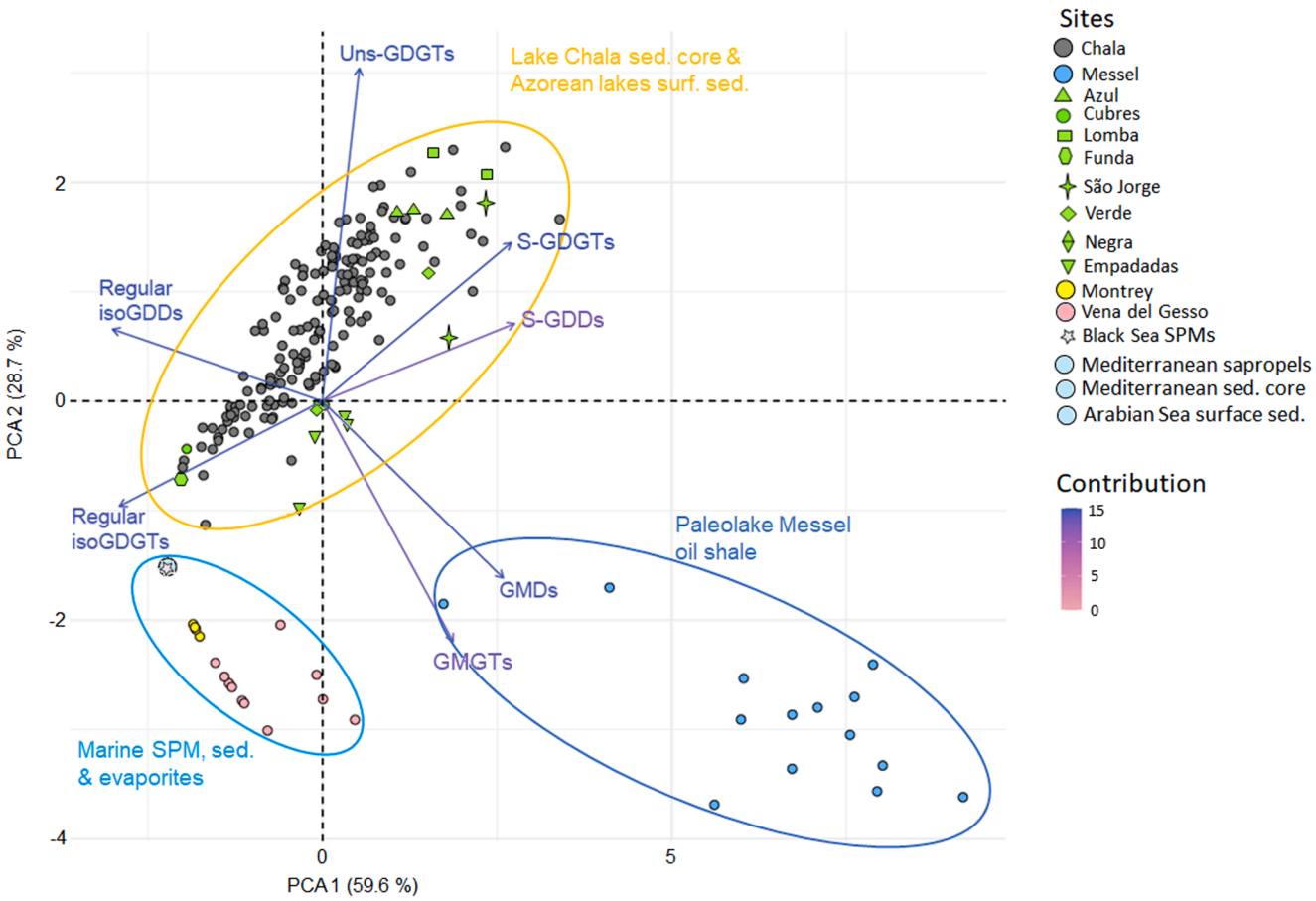


**Fig. 4.** PCA analysis of relative abundances of all identified GDGTs and GDDs in all investigated sediments (lacustrine, marine, hypersaline) grouped as unsaturated-, H-shaped (GMGT/GMD), regular- and S-shaped. The color code for the different GDGT and GDD groups and their contribution is indicated. Component score plot for PC1 and PC2 for the total of 259 core and surface sediments of 10 lakes, marine sediments, surface sediments, sapropels, evaporites and SPM combined (204 of which are lake sediments; 55 marine). Note: Lake Chala sediments plotted here include 14% turbidites (i.e sediments originating from a more peripheral location that end up at the drill site after bottom-slope failure) that were present in the investigated section of the core.

### 3.2. Distribution of isoprenoidal ether lipids

The relative abundance of the various classes of GDGTs and GDDs (regular, unsaturated, GMGTs and S-GDGTs) in the different sediments are summarized in Table 1. Regular GDGTs and regular GDDs were detected in all lacustrine and marine sediments with GDGTs dominating (84 to 95 % of total; Table 1; Fig. 3). *uns*-GDGTs (but no *uns*-GDDs) were detected in the Azorean lakes and Lake Chala (ca. 2 %) but not in the Messel oil shale and in the marine sediments. GMGTs were detected in the Messel oil shale sediments, the Miocene Monterey sediments, and the Vena del Gesso sediments (Table 1), while GMDs were only detected in the Messel oil shale sediments. S-GDGTs and S-GDDs were detected in all lacustrine sediments (Messel, Chala and the Azorean lakes) but not in the marine settings, with the exception of S-GDGTs that were present in two out of four Vena del Gesso beds investigated (beds VII and XI; Table 1). The detection of S-GDGTs in Messel oil shales was previously reported by Liu et al. (2016a). The average abundance of S-GDGTs (% of total GDGTs investigated in this study, Table 1) and S-GDDs (% of total GDDs investigated in this study, Table 1) were 7.2 ± 1.0 and 10.4 ± 1.4 respectively in Messel oil shales; 1.8 ± 0.3 and 5.9 ± 0.9 in the Azorean lakes surface sediments and 2.8 ± 0.1 and 2.1 ± 0.2 in Lake Chala sediments (Table 1; Fig. 3).

A PCA was performed on the data calculated from relative abundances of investigated GDGTs and GDDs to constrain the variability (Fig. 4). The first principal component (PCA1) accounts for 59.6 % of the total variance and the second (PCA2) for 28.7 % (Fig. 4) for 259 samples investigated (204 lacustrine and 55 marine). Regular GDGTs and GDDs were negatively loaded on the first principal component, while GMGTs, GMDs, S-GDGTs and S-GDDs were positively loaded. *uns*-GDGTs were positively loaded on the second principal component. All the Messel oil shales clustered in the same quadrant due to the relatively high abundance of GMGTs and GMDs. The Lake Chala sediment core samples and the majority of the Azorean lakes surface sediments clustered together, due to the presence of S-GDGTs. Most of the marine samples (Monterey, Vena del Gesso sediments, Black Sea SPM, Mediterranean sapropels and sediment core and Arabian Sea surface sediments) clustered in one quadrant. Overall, the PCA shows a clear division between the marine and lacustrine sediments based on ether lipid abundances, with a distinct difference between the Messel oil shale sediments and the other lacustrine samples.

### 3.3. Evaluation of ether lipids as indicators of lacustrine anoxia

#### 3.3.1. S-GDGTs and S-GDDs

Neither S-GDGTs nor S-GDDs were detected in any of the marine sediments, but they were present in the majority of the lacustrine sediments (Table 1). Previously, based on their presence in terrestrial sulfidic settings, Liu et al. (2016a) hypothesized that S-GDGTs are indicative of sulfidic conditions. This led Liu et al. (2016a) to suggest that S-GDGT-producing organisms may represent novel archaeal species which mediate the cycling of sulfur and terrestrial organic matter in coastal environments. However, the detection of S-GDGTs in the Azorean lakes, Messel oil shale sediments and Lake Chala sediments casts doubt on this hypothesis. For example, the Messel core section

investigated in this study corresponds to the Middle Messel-Formation, which was formed under anoxic–non-sulfidic conditions (Bauersachs et al., 2014). Deep Azorean lakes are monomictic and show seasonally induced water column stratification with bottom water anoxia during summer months (lakes Funda, Negra, Azul and Verde) (Fig. S3). Lakes Empadadas and São Jorge are lakes which are usually oxic throughout the year and Lake Cubres represents a coastal lagoon with one side more exposed to the Atlantic Ocean (sample SS6, West side; Table S1). On average, $S_{tot}$ was < 0.5 % (between 0.2 % in surface sediments of Lake Azul to 0.5 % in Lake Lomba), except for Lake Cubres (2.3 % on average), possibly due to the periodic inundations of the lake with seawater. These low sulfur contents make it unlikely that the bottom waters were euxinic. Some $H_2S$ can be produced in the water column of these lakes during the biological processes of sulphate reducing bacteria where available methane acts as electron-donor, as reported for other Azorean lakes by Tassi et al. (2018). Finally, the Lake Chala water column below 40 – 60 m is permanently stratified and anoxic (Wolff et al., 2011; Buckles et al., 2014), however with no evidence that anoxic bottom waters are sulfidic (e.g., low % of sulfur in sediment trap material, up to 1 %; Wolff et al., 2014). The same trap samples also show a positive correlation between sulfur and TOC ($R^2 = 0.80$), indicating that most sulfur is bound to organic matter (Wolff et al., 2014) making it highly unlikely that the remaining sulfur content was high enough to induce bottom water euxinia.

Interestingly, in Lakes Negra (SS1 and SS2) and Funda (SS1), which are deep lakes that have seasonally anoxic bottom waters, S-GDGTs and S-GDDs were not detected. This suggests that the archaeal producers of S-GDGTs and S-GDDs are found in lakes with anoxic bottom waters, but that anoxia does not guarantee their presence, and thus additional factors play a role in determining their production. In these deep, eutrophic lakes this could partly be due to a sharp gradient of physico-chemical properties in the water column (pH, dissolved oxygen, turbidity and nutrients; https://www.azores.gov.pt/Gra/srrn-drotrh/menus/principal/Monitorizacao/) that limits the niche for archaeal producer(s) of S-GDGTs and S-GDDs.

The absence of S-GDGTs and S-GDDs in nearly all marine sediments (Table 1) supports the previous hypothesis that they are produced by freshwater archaea (Liu et al., 2016a). However, we detected S-GDGTs in two beds of Vena del Gesso (VII and XI; Table 1), sediments deposited in an ancient evaporitic marine basin, with likely hypersaline conditions (Vai and Ricci Lucchi, 1977; Hsü et al., 1977). This fits with reported occurrence of S-GDGTs in salt marshes (Liu et al., 2016b) suggesting that S-GDGT producing archaea could be present in small saline lakes and evaporitic basins. Overall, our results suggest that S-GDGTs and S-GDDs are likely indicative of anoxic conditions (both intermittent and permanent) in lacustrine environments. Further studies are needed to determine their archaeal producer(s) and their biosynthetic pathway.

#### 3.3.2. Unsaturated GDGTs

Unsaturated GDGTs (*uns*-GDGTs) were reported in a suite of marine environments by Zhu et al. (2014) and based on their abundances and distributions, the authors suggested that they constitute an important archaeal lipid group in sediments deposited in euxinic basins and seep sites. Uns-GDGTs were also reported in a lacustrine environment (Fayetteville Green Lake surface sediment) by Liu et al. (2016a). Even though unsaturated diphytanyl glycerol diethers, such as archaeol, with multiple unsaturations (1–6) have been previously reported in *Halorubrum lacusprofundi* (a psychrotroph originally isolated from hypersaline Deep Lake in Antarctica; Gibson et al., 2005) and various halo(alkali) philic euryarchaeal strains isolated from hypersaline lakes (Bale et al., 2019b), *uns*-GDGTs are much more uncommon. For unsaturated diether lipids it was found that their proportion increases with increasing NaCl concentration in cultured halophilic archaea- which indicates that their biosynthesis represents a phenotypic adaptation (Maestrojuan et al., 1992; Hafenbradl et al., 1993; Dawson et al., 2012; Bale et al., 2019b). In this study, *uns*-GDGTs seem to be restricted to Lake Chala and almost all Azorean lakes (Table 1), while respective *uns*-GDDs were not detected. The presence of *uns*-GDGTs in the Azorean lakes coincides with the detection of S-GDGTs (with the exception of Lakes Negra and Funda, Fig. 3), and hence their presence in these settings may also be associated with low-oxygen conditions that occur during summer months. However, their absence in older samples, such as in Messel oil shales, suggests poor preservation potential for geological studies. Furthermore, their reported presence in marine systems (Zhu et al., 2014) introduces ambiguity to their association with lacustrine settings.

#### 3.3.3. GMGTs and GMDs

GMGTs, glycerol mono-alkyl glycerol tetraethers, also called H-GDGTs, were first identified in a hyperthermophilic methanogen and hypothesized to be an adaptation to heat stress in order to maintain membrane stability at high temperatures (Morii et al., 1998). Subsequently, GMGTs have been identified by Schouten et al. (2008a, b) in *Aciduliprofundum boonei* (obligate thermoacidophilic euryarchaeote) and a variety of marine and lacustrine sediments. More recently, GMGT-0 was reported in a sediment core from the New Jersey Shelf, USA (last 90 Myrs) (de Bar et al., 2019) and diverse GMGTs were detected in *Pyrococcus furiosus* (piezosensitive, hyperthermophilic archaeon) by Tourte et al. (2020). Naafs et al. (2018) reported GMGTs in globally distributed peatland soils. GMGTs were also detected in two peat cores from NE China (Tang et al., 2021). GMDs (glycerol monoalkene diol diethers) were reported in sediments deposited under hydrothermal conditions suggesting that (hyper)thermophilic Archaea may constitute a biological source (Bauersachs and Schwark, 2016). Liu et al. (2016b) reported GMD-0 in oil contaminated surface sediment from Guaymas Basin (Mexico) while de Bar et al. (2019) found it throughout a sediment core (New Jersey Shelf, USA) spanning last 90 Myrs.

In this study we detected GMGTs in lacustrine, marine and hypersaline environments, in agreement with their reported occurrence in a range of different lacustrine, marine (Schouten et al., 2008a, b; Liu et al., 2012b), and terrestrial settings (Naafs et al., 2018). However, GMDs were only detected in Messel oil shale sediments. Bauersachs and Schwark (2016) proposed that GMDs occur in hydrothermally affected environments, conditions which are not applicable for the Messel paleolake environment. It is more likely that, as was found for GMGTs (Schouten et al., 2008b), they can be synthesized by non-thermophilic archaea at low temperatures as well. More studies are needed to assess how widespread GMDs are in a variety of natural settings and what is their connection to respective GMGTs.

### 3.4. The relationship between GDGTs and GDDs

It has been postulated that GDDs are either degradation products of GDGTs or that they are biosynthesized by archaea, either as membrane components or as GDGT intermediates (Liu et al., 2012a; Yang et al., 2014; Meador et al., 2014; Coffinet et al., 2015; de Bar et al., 2019). We investigated the relationship between GDGTs and GDDs by first comparing the relative ring distributions of GDDs to those of GDGTs by calculating ring indices (RI; He et al. 2012) whereby we modified the RI equation to include the S-GDGTs and S-GDDs (section 2.6). The degree of cyclization of GDGTs exhibited a strong correlation with the degree of cyclization of GDDs (Fig. S4) irrespective of the sediment age. The strongest correlation was in the Lake Chala sediment core (n = 168) and the Azorean lake surface sediments (n = 18) (both $r^2 = 0.97$, Fig. S4). Similar distribution of rings in GDGTs and GDDs argues for a similar source and thus potentially a diagenetic conversion of GDGTs into GDDs.

We further examined this relationship by comparing the abundance (peak area/g sediment) of S-GDGTs with those of S-GDDs. We found strong positive correlations in the Messel oil shale sediment core (S-GDGT-1 vs S-GDD-1: $r^2 = 0.96$, n = 14 and S-GDGT-2 vs S-GDD-2: $r^2 = 0.92$, n = 14; Fig. 5) and in the Azorean lake surface sediments (S-GDGT-1 vs S-GDD-1: $r^2 = 0.79$, n = 14; Fig. 5), potentially suggesting a diagenetic origin of GDDs. However, S-GDDs in many samples were

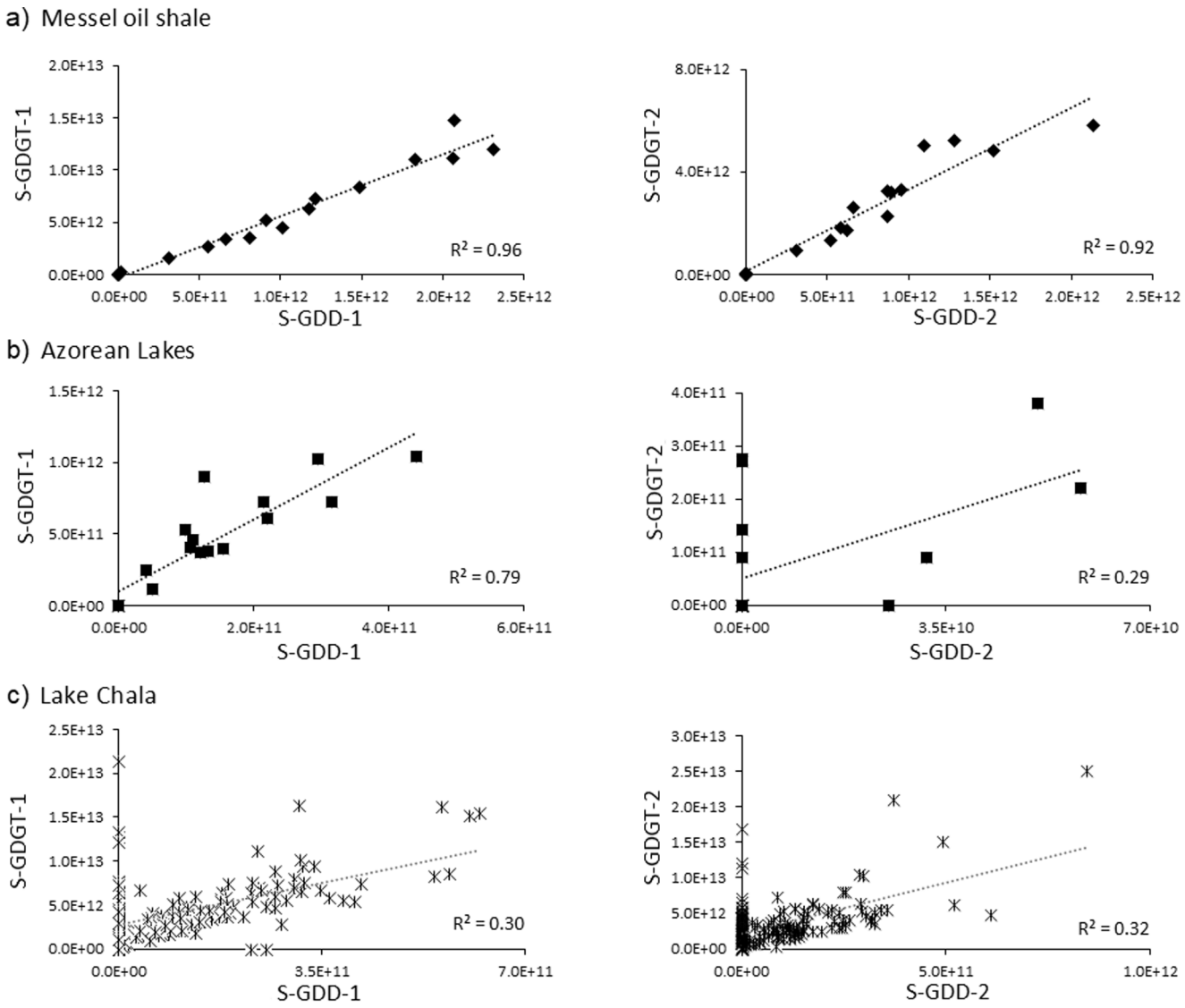


**Fig. 5.** Correlation graphs showing S-GDGT-1 vs S-GDD-1 and S-GDGT-2 vs S-GDD-2 (peak area per g sediment) in Messel oil shale sediment core (a), Azorean lake's surface sediments (b) and Lake Chala sediment core (c).

below detection level, leading to a poor correlation in the Azorean lakes (S-GDGT-2 vs S-GDD-2: $r^2 = 0.29$, n = 4, Fig. 5) and in the Lake Chala sediment core (S-GDGT-1 vs S-GDD-1, $r^2 = 0.30$, n = 112 and S-GDGT-2 vs S-GDD-2: $r^2 = 0.32$, n = 93; Fig. 5). Furthermore, GDD equivalents of *uns*-GDGTs as well as GMGTs were rarely found (Table 1). Finally, we did not observe an increase in GDDs versus GDGTs in the sediment cores of Lake Chala and Messel oil shale (Fig. S5) with depth as would be expected from a diagenetic conversion of GDGTs into GDDs and which has been observed previously (Yang et al., 2014). Therefore, it seems unlikely that GDDs are a direct diagenetic product of GDGTs. Overall, the observations from our study support the theory of a joint cellular origin for GDGTs and GDDs.

## 4. Conclusions

In this study we report a suite of isoprenoidal GDGTs and GDDs in modern and ancient lacustrine settings. Regular GDGTs and GDDs are the most abundant of all investigated isoprenoid lipids, while emphasis was on examining the potential of GMGTs, *uns*-GDGTs and newly reported S-GDGTs and their respective GDDs, as anoxia-related markers. GMDs were only detected in Messel oil shale, indicating they could be synthesized by non-thermophilic archaea much the same as GMGTs and show the same preservation potential in the geologic record. *Uns*-GDGTs were present in recent lacustrine settings (Azorean lakes and Lake Chala), both in surface sediments and in the core, while *uns*-GDDs could not be confidently identified. S-GDGTs and newly reported S-GDDs were detected in all lacustrine sediments which coupled with reports from previous studies on bottom water anoxia in these lakes, makes them potential indicators of low-oxygen or anoxic conditions. They were not detected in marine sediments and SPM with the exception of Vena del Gesso marls, which represent an example of an ancient hypersaline lagoonal system, indicating ability of S-producers to live in more saline conditions in an enclosed environment. Although their archaeal precursor(s) is/are not determined as of yet, we propose that the S-GDGTs and S-GDDs are produced in anoxic bottom waters of predominantly freshwater lakes, and in other stagnant water systems such as saline lagoons with established marine connection.

## Declaration of Competing Interest

The authors declare that they have no known competing financial interests or personal relationships that could have appeared to influence the work reported in this paper.

## Data availability

Data will be made available on request.

*Acknowledgements*

This work was carried out under the program of the Netherlands Earth System Science Centre (NESSC), financially supported by the Ministry of Education, Culture and Science (OCW).

Sample collection of surface sediments from the Azorean Lakes was funded under Luso-American Development Foundation grant (FLAD) to L. A. Zettler and by the Portuguese Science Foundation (FCT) (DL57/2016/ICETA/EEC2018/25) and the DISCOVERAZORES (PTDC/CTA-AMB/28511/2017) to P. M. V. R. Raposeiro. We are thankful to E. R. Zettler for his help in the Azorean sampling campaign. Sample collection and analysis of the Chala sediment core was co-financed by NESSC Gravitation Grant 024.002.001 from the Dutch Ministry of Education, Culture and Science (OCW) to J. S. Sinninghe Damsté, and by Ghent University Collaborative Research Operation grant BOF13/GOA/023 and Hercules infrastructure grant AUGE/15/14-G0H2916N from the Research Foundation of Flanders to D. Verschuren. We thank A. Mets from NIOZ for her work on extracting surface sediments from the Arabian Sea and core sediments from the Mediterranean. We are grateful to J. Riekenberg, D. Dorhout, M. Verweij and R. van Bommel at the Royal NIOZ for technical and analytical support. We furthermore thank D. Verschuren for his constructive feedback that helped improve the manuscript. Furthermore, the authors thank the editors and the reviewers for their helpful comments and feedback.

## Appendix A. Supplementary data

Supplementary data to this article can be found online at https://doi.org/10.1016/j.orggeochem.2023.104582.

## References

Auguet, J.C., Barberan, A., Casamayor, E., 2010. Global ecological patterns in uncultured Archaea. The International Society for Microbial Ecology 4, 182–190.

Bale, N.J., Hennekam, R., Hopmans, E.C., Dorhout, D., Reichart, G.-J., van der Meer, M., Villareal, T.A., Sinninghe Damsté, J.S., Schouten, S., 2019a. Biomarker evidence for nitrogen-fixing cyanobacterial blooms in a brackish surface layer in the Nile River plume during sapropel deposition. Geology 47, 1088–1092.

Bale, N.J., Sorokin, D.Y., Hopmans, E.C., Koenen, M., Rijpstra, W.I.C., Villanueva, L., Wienk, H., Sinninghe Damsté, J.S., 2019b. New Insights Into the Polar Lipid Composition of Extremely Halo(alkali)philic Euryarchaea From Hypersaline Lakes. Frontiers in Microbiology 10, 377.

Bale, N.J., Ding, S., Hopmans, E.C., Arts, M.G.I., Villanueva, L., Boschman, C., Haas, A.F., Schouten, S., Sinninghe Damsté, J.S., 2021. Lipidomics of environmental microbial communities. I: visualization of specific niches using untargeted analysis of high-resolution mass spectrometry data. Frontiers in Microbiology 2021, 659302.

Bauersachs, T., Schwark, L., 2016. Glycerol monoalkene diol diethers: a novel series of archaeal lipids detected in hydrothermal environments. Rapid Communication in Mass Spectrometry 30, 54–60.

Bauersachs, T., Schouten, S., Schwark, L., 2014. Characterization of the sedimentary organic matter preserved in Messel oil shale by bulk geochemistry and stable isotopes. Palaeogeography, Palaeoclimatology, Palaeoecology 410, 390–400.

Baxter, A.J., Hopmans, E.C., Russell, J.M., Sinninghe Damsté, J.S., 2019. Bacterial GMGTs in East African lake sediments: Their potential as palaeotemperature indicators. Geochimica et Cosmochimica Acta 259, 155–169.

Boetius, A., Ravenschlag, K., Schubert, C.J., Rickert, D., Widdel, F., Gieseke, A., Amann, R., Jørgensen, B.B., Witte, U., Pfannkuche, O., 2000. A marine microbial consortium apparently mediating anaerobic oxidation of methane. Nature 407, 623–626.

Bomberg, M., Montonen, L., Münster, U., Jurgens, G., 2008. Diversity and function of archaea in freshwater habitats. Current Trends in Microbiology 4, 61–89.

Brocks, J.J., Pearson, A., 2005. Building the Biomarker Tree of Life. Reviews in Mineralogy and Geochemistry 59, 233–258.

Buckles, L.K., Weijers, J.W.H., Verschuren, D., Sinninghe Damsté, J.S., 2014. Sources of core and intact branched tetraether membrane lipids in the lacustrine environment: anatomy of Lake Challa and its catchment, equatorial East Africa. Geochimica et Cosmochimica Acta 140, 106–126.

Buckles, L.K., Verschuren, D., Weijers, J.W.H., Cocquyt, C., Blaauw, M., Sinninghe Damsté, J.S., 2016. Interannual and (multi-)decadal variability in the sedimentary BIT index of Lake Challa, East Africa, over the past 2200 years: assessment of the precipitation proxy. Climate of the Past 12, 1243–1262.

Chappe, B., Michaelis, W., Albrecht, P., 1980. Molecular fossils of Archaebacteria as selective degradation products of kerogen. A.G. Douglas, J.R. Maxwell (Eds.). Advances in Organic Geochemistry Pergamon Press, Chichester, pp. 256–274.

Chappe, B. 1982. Fossiles Moléculaires d'Archaebacteries. PhD thesis, University of Strasbourg, France.

Coffinet, S., Huguet, A., Williamson, D., Bergonzini, L., Anquetil, C., Majule, A., Derenne, S., 2015. Occurrence and distribution of glycerol dialkanol diethers and glycerol dialkyl glycerol tetraethers in a peat core from SW Tanzania. Organic Geochemistry 83–84, 170–177.

Dawson, K.S., Freeman, K.H., Macalady, J.L., 2012. Molecular characterization of core lipids from halophilic archaea grown under different salinity conditions. Organic Geochemistry 48, 1–8.

de Bar, M.W., Rampen, S.W., Hopmans, E.C., Sinninghe Damsté, J.S., Schouten, S., 2019. Constraining the applicability of organic paleotemperature proxies for the last 90 myrs. Organic Geochemistry 128, 122–136.

De Long, E.F., 1992. Archaea in coastal marine environments. Proceedings of the National Academy of Sciences 89:5685–5689.

De Rosa, M., Gambacorta, A., 1988. The Lipids of Archaebacteria. Progress in Lipid Research 27, 153–175.

Ding, S., Bale, N.J., Hopmans, E.C., Villanueva, C., Arts, M.G.I., Schouten, S., Sinninghe Damsté, J.S., 2021. Lipidomics of environmental microbial communities. II: Characterization Using Molecular Networking and Information Theory. Frontiers in Microbiology 2021: doi.org/10.3389/fmicb.2021.659315.

Elling, F.J., Könneke, M., Lipp, J.S., Becker, K.W., Gagen, E.J., Hinrichs, K.-U., 2014. Effects of growth phase on the membrane lipid composition of thaumarchaeon Nitrosopumilus maritimus and their implications for archaeal lipid distributions in the marine environment. Geochimica et Cosmochimica Acta 141, 579–597.

Felder, M., Harms, F.J., 2004. Lithologie und genetische Interpretation der Forschungsbohrung Messel 2001. Courier Forschungsinstitut Senckenberg 252, 151–203.

Francis, C.A., Beman, J.M., Kuypers, M.M.M., 2007. New processes and players in the nitrogen cycle: the microbial ecology of anaerobic and archaeal ammonia oxidation. The International Society for Microbial Ecology 1, 19–27.

Franzen, J.L., Schaal, S., 2000. Der eozäne See von Messel. In: Meischner, D. (Ed.), Europäische Fossillagerstätten. Springer-Verlag, Berlin, pp. 177–183.

Fuhrman, J.A., McCallum, K., Davis, A.A., 1992. Novel major archaebacterial group from marine plankton. Nature 356, 148–149.

Gambacorta, A., Gliozzi, A., De Rosa, M., 1995. Archaeal lipids and their biotechnological applications. World Journal of Microbiology and Biotechnology 11, 115–131.

Gibson, J.A.E., Miller, M.R., Davies, N.W., Neill, G.P., Nichols, D.S., Volkman, J.K., 2005. Unsaturated diether lipids in the psychrotrophic archaeon Halorubrum lacusprofundi. Systematic and Applied Microbiology 28, 19–26.

Glissman, K., Chin, K.J., Casper, P., Conrad, R., 2004. Methanogenic pathway and archaeal community structure in the sediment of eutrophic Lake Dagow: effect of temperature. Microbial Ecology 48, 389–399.

Gonçalves, V., 2008. Contribuição do estudo das microalgas para a avaliação da qualidade ecológica das lagoas dos Açores: fitoplâncton e diatomáceas bentónicas. PhD thesis at Universidade dos Açores, Ponta Delgada (Portugal).

Grein, M., Utescher, T., Wilde, V., Roth-Nebelsick, A., 2011. Reconstruction of the middle Eocene climate of Messel using palaeobotanical data. Neues Jahrbuch für Geologie und Paläontologie 260, 305–318.

Hafenbradl, D., Keller, M., Thiericke, R., Stetter, K.O., 1993. A novel unsaturated archaeal ether core lipid from the hyperthermophile methanopyrus-kandleri. Systematic and Applied Microbiology 16, 165–169.

He, L., Zhang, C.L., Dong, H., Fang, B., Wang, G., 2012. Distribution of glycerol dialkyl glycerol tetraethers in Tibetan hot springs. Geoscience Frontiers 3, 289–300.

Hopmans, E.C., Schouten, S., Pancost, R.D., van der Meer, M.T.J., Sinninghe Damsté, J. S., 2000. Analysis of intact tetraether lipids in archaeal cell material and sediments by high performance liquid chromatography/atmospheric pressure chemical ionization mass spectrometry. Rapid Communications in Mass Spectrometry 14, 585–589.

Hsü, K., Montadert, L., Bernoulli, D., Cita, M.B., Erickson, A., Garrison, R.E., Kidd, R.B., Mèlierés, F., Müller, C., Wright, R., 1977. History of the Mediterranean salinity crisis. Nature 267, 399–403. http://www.azores.gov.pt/Gra/srrn-drotrh/menus/principal/Monitorização/.

Huguet, C., Fietz, S., Rosell-Melé, A., 2013. Global distribution patterns of hydroxyl glycerol dialkyl glycerol tetraethers. Organic Geochemistry 57, 107–118.

Inglis, G.N., Farnsworth, A., Lunt, D., Foster, G.L., Hollis, C.J., Pagani, M., Jardine, P.E., Pearson, P.N., Markwick, P., Galsworthy, A.M.J., 2015. Descent toward the Icehouse: Eocene sea surface cooling inferred from GDGT distributions. Paleoceanography 30, 1000–1020.

Isaacs, C.M., 1992. Geology handbook for the Cooperative Monterey Organic Geochemistry Study, Santa Maria and Santa Barbara-Ventura basins. California. Open-File Report. https://doi.org/10.3133/ofr92539E.

Isaacs, C. and Rullkötter, J., 2001. "Monterey Formation: from rock to molecules" Columbia University Press, New York, pp. 553.

Isaacs, C.M., Pollastro, R.M., Barron, J.A., Ingle Jr, J.C., Bukry, D., Dunbar, R.B., Keller, M.A., Tomson, J.H., Lewan, M.D., 2001. Geologic and paleontologic features of rock samples in the Monterey organic geochemistry study, Naples beach and Lions Head sections, California. "Monterey Formation: from rock to molecules" Columbia University Press, New York, Chapter 21, pp. 373.

Jarrell, K.F., Walters, A.D., Bochiwal, C., Borgia, J.M., Dickinson, T., Chong, J.P.J., 2011. Major players on the microbial stage: why archaea are important. Microbiology 157, 919–936.

Kassambara, A. and Mundt, F., 2020. Factoextra: Extract and Visualize the Results of Multivariate Data Analyses. R Package Version 1.0.7. https://CRAN.R-project.org/package=factoextra.
Kates, M., 1993. Biology of halophilic bacteria, Part, II. Membrane lipids of extreme halophiles: biosynthesis, function and evolutionary significance. Experientia 49, 1027–1036.
Knappy, C.S., Keely, B.J., 2012. Novel glycerol dialkanol triols in sediments: transformation products of glycerol dibiphytanyl glycerol tetraether lipids or biosynthetic intermediates? Chemical Communications 48, 841–843.
Knappy, C.S., Chong, J.P.J., Keely, B.J., 2009. Rapid discrimination of archaeal tetraether lipid cores by liquid chromatographytandem mass spectrometry. Journal of the American Society for Mass Spectrometry 20, 51–59.
Knappy, C.S., Nunn, C.E.M., Morgan, H.W., Keely, B.J., 2011. The major lipid cores of the archaeon Ignisphaera aggregans: implications for the phylogeny and biosynthesis of glycerol monoalkyl glycerol tetraether isoprenoid lipids. Extremophiles 15, 517–528.
Koga, Y., Morii, H., 2005. Recent Advances in Structural Research on Ether Lipids from Archaea Including Comparative and Physiological Aspects. Biochimica et Biophysica Acta 69, 2019–2034.
Koga, Y., Nishihara, M., Morii, H., Akagawa-Matsushita, M., 1993. Ether polar lipids of methanogenic bacteria: structures, comparative aspects, and biosyntheses. Microbiological Reviews 57, 164–182.
Könneke, M., Bernhard, A.E., de la Torre, J.R., Walker, C.B., Waterbury, J.B., Stahl, D.A., 2005. Isolation of an autotrophic ammonia-oxidizing marine archaeon. Nature 437, 543–546.
Kremer, A., Stein, R., Fahl, K., Ji, Z., Yang, Z., Wiers, S., Matthiessen, J., Forwick, M., Löwemark, L., O'Regan, M., Chen, J., Snowball, I., 2018. Changes in sea ice cover and ice sheet extent at the Yermak Plateau during the last 160 ka – reconstructions from biomarker records. Quaternary Science Reviews 182, 93–108.
Langworthy, T.A., 1977. Long-chain diglycerol tetraethers from Thermoplasma acidophilum. Biochimica et Biophysica Acta - Lipids and Lipid Metabolism 487, 37–50.
Lengger, S.K., Hopmans, E.C., Reichart, G.-J., Nierop, K.G.J., Sinninghe Damsté, J.S., Schouten, S., 2012. Intact polar and core glycerol dibiphytanyl glycerol tetraether lipids in the Arabian Sea oxygen minimum zone. Part II: Selective preservation and degradation in sediments and consequences for the TEX86. Geochimica et Cosmochimica Acta 98, 244–258.
Lenz, O.K., Wilde, V., Riegel, W., 2011. Short-term fluctuations in vegetation and phytoplankton during the Middle Eocene greenhouse climate: a 640-kyr record from the Messel oil shale (Germany). The International Journal of Earth Sciences 100, 1851–1874.
Lipp, J.S., Hinrichs, K.-U., 2009. Structural diversity and fate of intact polar lipids in marine sediments. Geochimica et Cosmochimica Acta 73, 6816–6833.
Liu, X.-L., Birgel, D., Elling, F.J., Sutton, P.A., Lipp, J.S., Zhu, R., Zhang, C., Könneke, M., Peckmann, J., Rowland, S.J., Summons, R.E., Hinrichs, K.-U., 2016a. From ether to acid: a plausible degradation pathway of glycerol dialkyl glycerol tetraethers. Geochimica et Cosmochimica Acta 183, 138–152.
Liu, X.-L., De Santiago Torio, A., Bosak, T., Summons, R.E., 2016b. Novel archaeal tetraether lipids with a cyclohexyl ring identified in Fayetteville Green Lake, NY, and other sulfidic lacustrine settings. Rapid Communications in Mass Spectrometry 30, 1197–1205.
Liu, R., Han, Z., Zhao, J., Zhang, H., Li, D., Ren, J., Pan, J., Zhang, H., 2020. Distribution and source of glycerol dialkyl glycerol tetraethers (GDGTs) and the applicability of GDGT-based temperature proxies in surface sediments of Prydz Bay, East Antarctica. Polar Research 39. https://doi.org/10.33265/polar.v39.3557.
Liu, X.-L., Lipp, J.S., Schröder, J.M., Summons, R.E., Hinrichs, K.-U., 2012a. Isoprenoid glycerol dialkanol diethers: a series of novel archaeal lipids in marine sediments. Organic Geochemistry 43, 50–55.
Liu, X.-L., Lipp, J.S., Simpson, J.H., Lin, Y.-S., Summons, R.E., Hinrichs, K.-U., 2012b. Mono- and dihydroxyl glycerol dibiphytanyl glycerol tetraethers in marine sediments: Identification of both core and intact polar lipid forms. Geochimica et Cosmochimica Acta 89, 102–115.
Liu, X.-L., Summons, R.E., Hinrichs, K.-U., 2012c. Extending the known range of glycerol ether lipids in the environment: structural assignments based on tandem mass spectral fragmentation patterns. Rapid Communications in Mass Spectrometry 26, 1–8.
Lü, X., Liu, X., Xu, C., Song, J., Li, X., Yuan, H., Li, N., Wang, D., Yuan, H., Ye, S., 2019. The origins and implications of glycerol ether lipids in China coastal wetland sediments. Scientific Reports 9, 18529.
Maestrojuan, G.M., Boone, J.E., Mah, R.A., Menaia, J.A.G.F., Sachs, M.S., Boone, D.R., 1992. Taxonomy and halotolerance of mesophilic Methanosarcina strains, assignment of strains to species, and synonymy of Methanosarcina mazei and Methanosarcina frisia. International Journal of Systematic and Evolutionary Microbiology 42, 561–567.
Maitituerdi, A., Van Daele, M., Verschuren, D., De Batist, M., Waldmann, N., 2022. Depositional history of Lake Chala (Mt. Kilimanjaro, equatorial East Africa) from high-resolution seismic stratigraphy. Journal of African Earth Sciences 189, 104499.
Martin-Jones, C., Lane, C., Van Daele, M., Van Der Meeren, T., Wolff, C., Moorhouse, H., Tomlinson, E., Verschuren, D., 2020. History of scoria-cone eruptions on the eastern shoulder of the Kenya-Tanzania Rift revealed in the 250-ka sediment record of Lake Chala near Mount Kilimanjaro. Journal of Quaternary Science 35, 245–255.
Matthess, G., 1966. Zur Geologie des Ölschiefervorkommens von Messel bei Darmstadt. Abhandlungen des Hessischen Landesamtes für Bodenforschung 51, 87.
Meador, T.B., Zhu, C., Elling, F.J., Könneke, M., Hinrichs, K.-U., 2014. Identification of isoprenoid glycosidic glycerol dibiphytanol diethers and indications for their biosynthetic origin. Organic Geochemistry 69, 70–75.
Mertz, D.F., Renne, P.R., 2005. A numerical age for the Messel fossil deposit (UNESCO World Heritage Site) derived from 40Ar/39Ar dating on a basaltic rock fragment. Courier Forschungsinstitut Senckenberg 255, 67–75.
Morii, H., Eguchi, T., Nishihara, M., Kakinuma, K., Konig, H., Koga, Y., 1998. A novel ether core lipid with H-shaped C-80-isoprenoid hydrocarbon chain from the hyperthermophilic methanogen Methanothermus fervidus. Biochimica et Biophysica Acta 1390, 339–345.
Naafs, B.D.A., McCormick, D., Inglis, G., Pancost, R.D. and the T-GRES peat database collaborators, 2018. Archaeal and bacterial H-GDGTs are abundant in peat and their relative abundance is positively correlated with temperature. Geochimica et Cosmochimica Acta 227, 156–170.
O'Brien, C.L., Robinson, S.A., Pancost, R.D., Sinninghe Damsté, J.S., Schouten, S., Lunt, D.J., Alsenz, H., Bornemann, A., Bottini, C., Brassell, S.C., Farnsworth, A., Forster, A., Huber, B.T., Inglis, G.N., Jenkyns, H.C., Linnert, C., Littler, K., Markwick, P., McAnena, A., Mutterlose, J., Naafs, B.D.A., Püttmann, W., Sluijs, A., van Helmond, N.A.G.M., Vellekoop, J., Wagner, T., Wrobel, N.E., 2017. Cretaceous sea-surface temperature evolution: Constraints from TEX86 and planktonic foraminiferal oxygen isotopes. Earth-Science Reviews 172, 224–247.
Pancost, R.D., Hopmans, E.C., Sinninghe Damsté, J.S., the MEDINAUT Shipboard Scientific Party, 2001. Archaeal lipids in Mediterranean cold seeps: molecular proxies for anaerobic methane oxidation. Geochimica et Cosmochimica Acta 65, 1611–1627.
Porteiro, J., 2000. Lagoas dos Açores. Elementos de Suporte ao Planeamento Integrado. Universidade dos Açores, Ponta Delgada, pp. 344.
Raposeiro, P.M., Sáez, A., Giralt, S., Costa, A.C., Gonçalves, V., 2018. Causes of spatial distribution of subfossil diatom and chironomid assemblages in surface sediments of a remote deep island lake. Hydrobiologia 815, 141–163.
Ribeiro, D.C., Martins, G., Nogueira, R., Brito, A.G., 2014. Mineral cycling and pH gradient related with biological activity under transient anoxic−oxic conditions: effect on P mobility in volcanic lake sediments. Environmental Science & Technology 48, 9205–9210.
Ritter, C., Gonçalves, V., Pla-Rabes, S., de Boer, E.J., Bao, R., Sáez, A., Hernández, A., Sixto, M., Richter, N., Benavente, M., Prego, R., Giralt, S., Raposeiro, P.M., 2022. The vanishing and the establishment of a new ecosystem on an oceanic island – Anthropogenic impacts with no return ticket. Science of the Total Environment 830, 154828.
Rullkötter, J., Littke, R., Hagedorn-Götz, I., Jankowski, B., 1988. Vorläufige Ergebnisse der organisch-geochemischen Untersuchungen an Kernproben des Messeler Ölschiefers. - Der eozäne Messelsee - Eocene Lake Messel (Franzen, J.L. & Michaelis, W., eds Courier Forschungsinstitut Senckenberg 107, 37–51.
Rush, D., Talbot, H.M., van der Meer, M.T.J., Hopmans, E.C., Douglas, B., Sinninghe Damsté, J.S., 2019. Biomarker evidence for the occurrence of anaerobic ammonium oxidation in the eastern Mediterranean Sea during Quaternary and Pliocene sapropel formation. Biogeosciences 16, 2467–2479.
Schouten, S., de Loureiro, M.R.B., Sinninghe Damsté, J.S., de Leeuw, J.W., 2000b. Molecular biogeochemistry of Monterey sediments, Naples Beach, California I: Distributions of hydrocarbons and organic sulphur compounds. The Monterey Formation: From Rock to Molecule, Colombia University Press, New York, pp 150–174.
Schouten, S., Hopmans, E.C., Pancost, R.D., Sinninghe Damsté, J.S., 2000b. Widespread occurrence of structurally diverse tetraether membrane lipids: evidence for the ubiquitous presence of low-temperature relatives of hyperthermophiles. Proceedings of the National Academy of Sciences 97, 14421–14426.
Schouten, S., Schoell, M., Sinninghe Damsté, J.S., Summons, R.E., de Leeuw, J.W., 2000c. Molecular biogeochemistry of Monterey sediments, Naples Beach, California, II: Stable carbon isotopic compositions of free and sulfur-bound carbon skeletons. In: The Monterey Formation: From Rocks to Molecules. Columbia University Press, New York., pp. 175–188
Schouten, S., Hopmans, E.C., Schefuß, E., Sinninghe Damsté, J.S., 2002. Distributional variations in marine crenarchaeotal membrane lipids: a new tool for reconstructing ancient sea water temperatures? Earth and Planetary Science Letters 204, 265–274.
Schouten, S., Baas, M., Hopmans, E.C., Reysenbach, A.-L., Sinninghe Damsté, J.S., 2008a. Tetraether membrane lipids of Candidatus "Aciduliprofundum boonei", a cultivated obligate thermoacidophilic euryarchaeote from deep-sea hydrothermal vents. Extremophiles 12, 119–124.
Schouten, S., Baas, M., Hopmans, E.C., Sinninghe Damsté, J.S., 2008b. An unusual isoprenoid tetraether lipid in marine and lacustrine sediments. Organic Geochemistry 39, 1033–1038.
Sinninghe Damsté, J.S., Frewin, N.L., Kenig, F., de Leeuw, J.W., 1995. Molecular indicators for paleoenvironmental changes in a Messinian evaporitic sequence (Vena del Gesso, Italy). I: Variations in extractable organic matter of ten cyclically deposited marl beds. Organic Geochemistry 23, 471–483.
Sinninghe Damsté, J.S., Schouten, S., Hopmans, E.C., van Duin, A.C.T., Geenevasen, J.A. J., 2002. Crenarchaeol: the characteristic core glycerol dibiphytanyl glycerol tetraether membrane lipid of cosmopolitan pelagic crenarchaeota. Journal of Lipid Research 43, 1641–1651.
Spang, A., Caceres, E.F., Ettema, T.J.G., 2017. Genomic exploration of the diversity, ecology, and evolution of the archaeal domain of life. Science 357, 6351. https://doi.org/10.1126/science.aaf3883.
Sturt, H.F., Summons, R.E., Smith, K., Elvert, M., Hinrichs, K.-U., 2004. Intact polar membrane lipids in prokaryotes and sediments deciphered by high performance liquid chromatography/electrospray ionization multistage mass spectrometry - new biomarkers for biogeochemistry and microbial ecology. Rapid Communication in Mass Spectrometry 18, 617–628.
Summons, R.E., Welander, P.V., Gold, D.A., 2021. Lipid biomarkers: molecular tools for illuminating the history of microbial life. Nature Reviews Microbiology 20, 174–185.

Tang, X., Naafs, B.D.A., Pancost, R.D., Liu, Z., Fan, T., Zheng, Y., 2021. Exploring the influences of temperature on "H-shaped" glycerol dialkyl glycerol tetraethers in a stratigraphic context: evidence from two peat cores across the Late Quaternary. Frontiers in Earth Science 8, 477.

Tassi, F., Cabassi, J., Andrade, C., Callieri, C., Silva, C., Viveiros, F., Corno, G., Vaselli, O., Selmo, E., Gallorini, A., Ricci, A., Giannini, L., Cruz, J.V., 2018. Mechanisms regulating $CO_2$ and $CH_4$ dynamics in the Azorean volcanic lakes (São Miguel island, Portugal): Bio-Geochemistry of Volcanic Lakes in the Azores, Portugal. Journal of Limnology 77. https://doi.org/10.4081/jlimnol.2018.1821.

Thompson, D.H., Wong, K.F., Humphry-Baker, R., Wheeler, J.J., Shankar, J.M.K., Rananavare, B., 1992. Tetraether bolaform amphiphiles as models of archaebacterial membrane lipids: Raman spectroscopy, 31P NMR, X-ray scattering and electron microscopy. Journal of the American Chemical Society 114, 9035–9042.

Tourte, M., Kuentz, V., Schaeffer, P., Grossi, V., Cario, A., Oger, P., 2020. Novel intact polar and core lipid compositions in the Pyrococcus model species, P. furiosus and P. yayanosii, reveal the largest lipid diversity amongst Thermococcales. Biomolecules 10, 830.

Vai, G.B., Ricci Lucchi, F., 1977. Algal crusts, autochthonous and clastic gypsum in a cannibalistic evaporite basin; a case history from the Messinian of Northern Apennine. Sedimentology 24, 211–244.

Verschuren, D., Sinninghe Damsté, J.S., Moernaut, J., Kristen, I., Blaauw, M., Fagot, M., Haug, G., CHALLACEA project members, 2009. Half-precessional dynamics of monsoon rainfall near the East African Equator. Nature 462, 637–641.

Verschuren, D., Olago, D.O., Rucina, S.M., Odhengo, P.O. and on behalf of the ICDP DeepCHALLA Consortium, 2013. DeepCHALLA: Two glacial cycles of climate and ecosystem dynamics from equatorial East Africa. Scientific Drilling 15: 72–76.

Vuillemin, A., Ariztegui, D., Horn, F., Kallmeyer, J., Orsi, W.D. and the PASADO Science Team, 2018. Microbial community composition along a 50 000-year lacustrine sediment sequence. FEMS Microbiology Ecology 94, fiy029, https://doi.org/10.1093/femsec/fiy029.

Weiss, G.M., Schouten, S., Sinninghe Damsté, J.S., van der Meer, M.T.J., 2019. Constraining the application of hydrogen isotopic composition of alkenones as a salinity proxy using marine surface sediments. Geochimica et Cosmochimica Acta 250, 34–48.

Wolff, C., Haug, G.H., Timmermann, A., Sinninghe Damsté, J.S., Brauer, A., Sigman, D. M., Cane, M.A., Verschuren, D., 2011. Reduced interannual rainfall variability in East Africa during the last ice age. Science 333, 743–747.

Wolff, C., Kristen-Jenny, I., Schettler, G., Plessen, B., Meyer, H., Dulski, P., Naumann, R., Brauer, A., Verschuren, D., Haug, G.H., 2014. Modern seasonality in Lake Challa (Kenya/Tanzania) and its sedimentary documentation in recent lake sediments. Limnology and Oceanography 59. https://doi.org/10.4319/lo.2014.59.5.1621.

Wörmer, L., Lipp, J.S., Schröder, J.M., Hinrichs, K.-U., 2013. Application of two new LC–ESI–MS methods for improved detection of intact polar lipids (IPLs) in environmental samples. Organic Geochemistry 59, 10–21.

Wörmer, L., Lipp, J.S., Hinrichs, K.-U., 2015. Comprehensive analysis of microbial lipids in environmental samples through HPLC-MS protocols. In: McGenity, T., Timmis, K., Nogales, B. (Eds.), Hydrocarbon and Lipid Microbiology Protocols. Springer Protocols Handbooks, Springer, Berlin, Heidelberg, pp. 289–317.

Yang, H., Pancost, R.D., Tang, C., Ding, W., Dang, X., Xie, S., 2014. Distributions of isoprenoid and branched glycerol dialkanol diethers in Chinese surface soils and a loess paleosol sequence: implications for the degradation of tetraether lipids. Organic Geochemistry 66, 70–79.

Zhu, C., Yoshinaga, M.Y., Peters, C.A., Liu, X.-L., Elvert, M., Hinrichs, K.-U., 2014. Identification and significance of unsaturated archaeal tetraether lipids in marine sediments. Rapid Communication in Mass Spectrometry 28, 1144–1152.